

## Bifurcations of a Forced Magnetic Oscillator near Points of Resonance

Paul Bryant and Carson Jeffries

*Department of Physics, University of California, Berkeley, California 94720, and  
Materials and Molecular Research Division, Lawrence Berkeley Laboratory, Berkeley, California 94720*

(Received 17 April 1984)

We study a forced symmetric oscillator containing a saturable inductor with magnetic hysteresis, approximated by a noninvertible map of the plane. The system displays a Hopf bifurcation to quasiperiodicity, entrainment horns, and chaos. Behavior near points of resonance (weak and strong) is found to correspond well with Arnold's theory. Within an entrainment horn, we observe symmetry breaking, period doubling, and complementary band merging. The symmetry behavior is explained by use of the concept of a half-cycle map.

PACS numbers: 47.25.-c, 05.20.-y, 05.40.+j

The nonlinear dynamics of a driven oscillator is central to the understanding of physical systems which can be viewed as a collection of coupled oscillators or modes. We report here the dynamics exhibited by a driven, nonlinear, symmetric oscillator containing a toroidal ferromagnetic core with saturation and hysteresis. This simple system shows a rich variety of behavior as a function of control parameters, typically the amplitude and period of the driving oscillator. Much of this behavior occurs in conjunction with a Hopf bifurcation to quasiperiodic motion and includes multiple attractors associated with strong resonances, spontaneous symmetry-breaking bifurcations, entrainment horns, saddle-node and homoclinic bifurcations, cascades of period-doubling bifurcations, complementary band merging, and crises of the attractor. Using a novel method of transient analysis following repeated initializations of the system, we can observe structure in the Poincaré section that is usually hidden, such as unstable fixed points, stable and unstable manifolds of saddle points, and the boundaries of the basins of attraction. In the case of strong resonance we demonstrate remarkable correspondence between experiment and theory.<sup>1-5</sup>

The system consists of four elements connected in parallel: (1) an oscillating current source,  $I_S(t) = I_0 \cos \omega_1 t$ ; (2) a linear negative resistance<sup>6</sup>  $R$ ; (3) a capacitance  $C$ ; and (4) a nonlinear inductor.<sup>7</sup> The system is weakly self-oscillating at frequency  $\omega_2$  while being forced at  $\omega_1 = 2\pi/\tau$ . We usually fix  $R$  and  $C$  and measure the inductor current  $I_L(t)$  and voltage  $V_L(t)$  for some setting of  $\tau$  and  $I_{\text{rms}} = I_0\sqrt{2}$ . Poincaré sections are  $I_L$  vs  $I_S$  strobed when  $V_L = 0$ .

One easily obtains, using Kirchhoff's laws, the equation  $(l/n)H = I_S(t) - (nA/R)\dot{B} - nAC\ddot{B}$  (SI units), where  $l$  = magnetic path length (0.1097 m),  $A$  = effective core cross section ( $1.51 \times 10^{-5}$  m<sup>2</sup>),  $n$  = number of turns (100),  $H$  = magnetic field, and  $B$  = magnetic induction. At sufficiently low fre-

quencies, so that the core is in quasiequilibrium, there will be some monotonic relation between  $B$  and  $H$  and this relation will change (because of magnetic hysteresis) whenever  $\dot{B}$  changes sign. The resultant equation of motion is irreversible. As  $B$  is changed continuously in one direction, it will approach the characteristic saturation-hysteresis loop. For oscillations which nearly saturate in both directions we make the approximations that  $H(B)$  merges completely each time with the saturation loop and that  $H(B)$  will depend solely on the value of  $B$  (or  $H$ ) at the most recent turning point. In this case the state of the system at a turning point is given by two variables, one representing the core (e.g.,  $I_L$ ) and one representing the phase of the driver (e.g.,  $I_S$ ). Hence, in such a case the motion is governed by a *noninvertible* map of the plane. This noninvertibility has been observed experimentally through initialization, as well as in a numerical solution of the equation using an empirical  $H(B)$  relation.

Our method of initialization takes advantage of this approximation to a map of the plane by setting the initial  $I_L$  and  $I_S$  at a turning point of  $B$ . An electronic switch is used to force the system into a stable oscillation whose amplitude and phase [with respect to  $I_S(t)$ ] are adjustable. Deactivating the switch at a turning point initializes the system and a transient leading to an attractor is observed. By adjusting this initializer (and hence varying the initial conditions) we can look for fixed points and other structures in the Poincaré space. The stable and unstable manifolds of a saddle point may be traced out by initializing on its stable manifold. System noise randomly determines the trajectory leaving the saddle, and repeated initializations will cover its unstable manifold completely [see Fig. 1(a)].

The data in Fig. 2 summarize the behavior in the  $(\tau, I_{\text{rms}})$  parameter space where the Hopf bifurcation ( $H$ ) occurs. Below the line  $H$  there is a symmetric oscillation [ $I_L(t) = -I_L(t + \tau/2)$ ] denoted

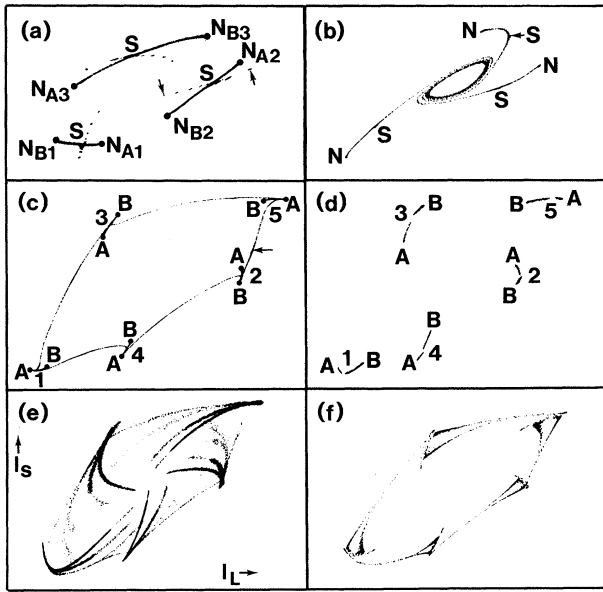


FIG. 1. Poincaré sections in  $(I_L, I_S)$  strobed at  $V_L = 0$ . (a) Period-3 saddle point ( $S$ ) located by initializing repeatedly on its stable manifold. Two initialization points (arrows) were used. The complementary saddle is not seen with this initialization, but the complementary period-3 attracting nodes ( $N_A$  and  $N_B$ ) are both shown. This is in the  $4/3$  horn for which  $q = 6$ . (b) Region  $b_1$  of Fig. 3(a). Initialized repeatedly near period-3 saddle (arrow), shows unstable manifolds going in to invariant circle and out to period-3 node. (c) In  $7/5$  horn, Fig. 4, following spontaneous symmetry breaking, shows  $A$  and  $B$  attractors and iteration sequence. Initialized repeatedly near saddle point (arrow). (d) Just prior to complementary band merging, shows both attractors using a double exposure. (e) Just after interior crisis, each piece of the attractor has suddenly increased in size contacting the adjacent piece. (f) The attractor just outside the horn boundary where symmetry-broken nodes and saddles have annihilated.

$1/1$ . As  $H$  is crossed, a two-torus emerges from this orbit on which the motion is quasiperiodic. This appears as a circle in the Poincaré section. The orbit winds around this torus at the new frequency  $\omega_2$ . The state of the system on the torus can be expressed  $X = X(\theta_1, \theta_2)$  where  $\theta_1 = \omega_1 t$  and  $\theta_2 = \omega_2 t$ . This motion has Fourier components at  $\omega_{ij} = i\omega_1 + j\omega_2$ . Symmetric variables (e.g.,  $I_L, V_L, B$ ) on a symmetric torus satisfy  $X(\theta_1, \theta_2) = -X(\theta_1 + \pi, \theta_2 + \pi)$  which requires that  $i + j$  be odd. Entrainment (frequency locking) occurs within the horn-shaped regions of Fig. 2, with  $\omega_2/\omega_1 = M/N$  as indicated. The horns emerge from the line  $H$  at points of resonance—where the Poincaré map has a fixed point whose complex conjugate eigenvalues are roots of unity. Associated with each resonance

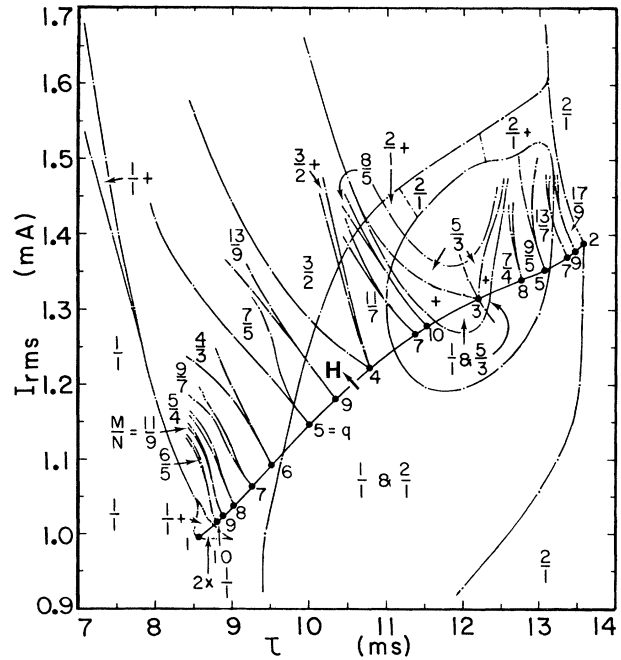


FIG. 2.  $(\tau, I_{rms})$  parameter space with  $R = -500 \Omega$  and  $C = 7.5 \mu F$ . Entrainment domains labeled by frequency ratio  $M/N$ , points of resonance by order  $q$  (for  $q \leq 10$ ), Hopf bifurcation by  $H$ . Portions of entrainment domains labeled " $M/N+$ " have coexisting quasiperiodic attractors. The " $5/3+$ " regions are labeled with "+" alone. In some regions two entrained attractors coexist, e.g., the region labeled  $1/1$  and  $5/3$ . The region labeled  $2 \times 1/1$  has two distinct  $1/1$  type attractors. Hysteresis is observed when these multiple-attractor regions are traversed.

is an order  $q$  which gives the rotational symmetry of the map near the fixed point. Nearby transient orbits wind around the bifurcating resonant orbit and close (in first order) after winding  $M$  times around during  $N$  cycles of  $\omega_1$ . A nearby orbit passing through  $(\theta_1, \theta_2)$  will also pass through  $(\theta_1 + \pi, \theta_2 + \pi)$  if  $M$  and  $N$  are odd. This orbit is symmetrical [ $I_L(t) = -I_L(t + N\tau/2)$ ] and  $q = N = \text{odd}$ . When  $M$  or  $N$  is even, the orbit is asymmetrical and a complementary orbit passes through  $(\theta_1 + \pi, \theta_2 + \pi)$  doubling the rotational symmetry, i.e.,  $q = 2N = \text{even}$ , and the associated entrainment horn always has complementary attractors [Fig. 1(a)]. Note that a pair of  $2/1$  attractors coexist with other attractors in a large region of Fig. 2.

For  $1 \leq q \leq 4$  (strong resonance) complicated bifurcation patterns occur, usually accompanied by hysteresis. For  $q = 3$ , Fig. 3(a) shows many regions ( $a_1, a_2, \dots$ ) and Fig. 3(b) shows schematically the Poincaré sections observed by initialization [see, e.g., Fig. 1(b)] for each region.

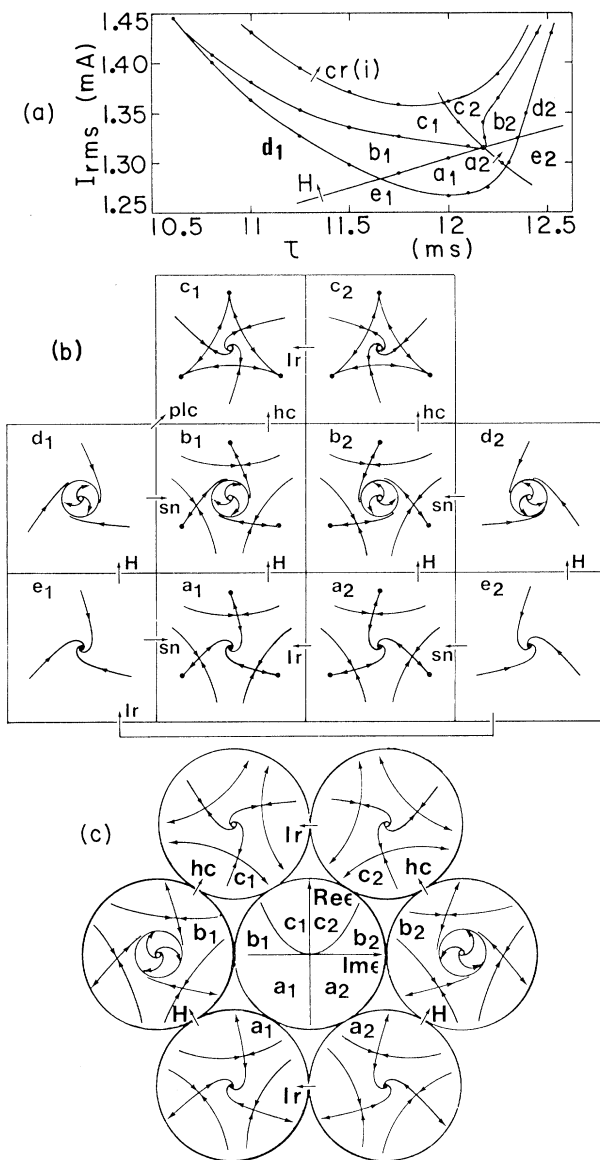


FIG. 3. (a) Regions of Fig. 2 near  $q=3$  point.  $H$ , Hopf bifurcation,  $cr(i)$ , interior crisis. (b) Typical Poincaré section observed for each region showing periodic sinks (solid dots), sources (open dots), saddles (identified by crossing manifold lines), and invariant circles. Bifurcations:  $H$ , Hopf;  $hc$ , homoclinic (circle annihilates on contact with saddles);  $lr$ , left spiral to right spiral;  $sn$ , saddle node;  $plc$ , phase-locked circle (saddles and nodes appear on pre-existing circle). (c) Theoretical  $q=3$  bifurcation diagram (Ref. 1).  $\epsilon$  is a complex parameter equivalent to two real parameters.

Behavior near points of resonance is discussed theoretically by Arnold,<sup>1-3</sup> Iooss,<sup>4</sup> and Takens.<sup>5</sup> Arnold uses the method of averaging in Siefert's foliation to obtain a vector field in the plane which describes the behavior of the Poincaré map near the

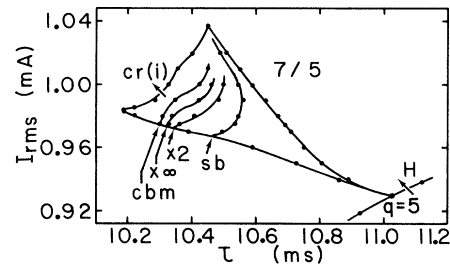


FIG. 4.  $7/5$  entrainment horn showing internal bifurcations in  $(\tau, I_{rms})$  space with  $R = -392 \Omega$  and  $C = 7.5 \mu F$ .  $sb$ , symmetry breaking:  $\times 2$ , period doubling;  $\times \infty$ , end of  $\times 2$  cascade;  $cbm$ , complementary band merging;  $cr(i)$ , interior crisis.

point of resonance.<sup>1</sup> The resultant "principal equation" has rotational symmetry through the angle  $2\pi/q$ . For  $q > 4$  (weak resonance) there is always an entrainment horn like those in Fig. 1 in which  $q$  nodes alternate with  $q$  saddles on a phase-locked circle.

Figure 3(c) gives the theoretical bifurcation diagram for  $q=3$ , adapted from Arnold.<sup>1</sup> The observed period-3 nodes, present in  $a_1, a_2, b_1, b_2, c_1$ , and  $c_2$  of Fig. 3(b) are not involved in the bifurcation of the resonant fixed point. Although they do not appear in Fig. 3(c), the presence of another attractor must be inferred from the unstable manifolds that go off to infinity. The period-3 nodes appear via saddle-node bifurcation as shown in  $d_1, e_1, \dots$ . Data on other cases of strong resonance behave similarly. One of our principal findings is the remarkably good correspondence between data and theory.

Figure 4 shows the bifurcations within an entrainment horn ( $7/5$ ) of the symmetrical type. First there is a symmetry-breaking bifurcation [Fig. 1(c)], followed by a cascade of period-doubling bifurcations to chaos. Then there is a sequence of band mergings of the attractor followed by a complementary band merging where the complementary attractors connect and symmetry is restored [Fig. 1(d)]. At the upper boundary of the horn an interior crisis<sup>8</sup> occurs when the period-5 attractor contacts its interior-basin boundary and phase locking is lost [Fig. 1(e)]. Note that the bifurcation lines may intersect the horn boundary. In this case the saddle points (with which the nodes annihilate) also bifurcate [Fig. 1(f)]. The bifurcations just described also occur in cases of strong resonance. In Fig. 3(a) only the interior crisis line is shown, but the other bifurcations also occur.

We can explain some of this behavior by the following argument. In a symmetrical system where every state  $X$  has a complement  $X'$  we can define a

complementary Poincaré section as the intersection of the orbit with the complement of the original Poincaré space. If  $F_+(X)$  maps from the original to the subsequent point in the complement, then its complement  $F'_+(X)$  is a half-cycle map<sup>9</sup> whose second iterate is the Poincaré map. When the system exhibits complementary attractors,  $F'_+(X)$  iterates back and forth between them and consequently a symmetry-breaking bifurcation is just the first period-doubling bifurcation for the half-cycle map. Similarly, complementary band merging is just the final band merging of the half-cycle map. The symmetry-breaking bifurcation of Fig. 1(c) occurs when one of the eigenvalues of the linearized  $q$ th iterate of the half-cycle map for the period- $q$  node crosses  $-1$ . In our system this occurs while the other eigenvalue is still positive, indicating that one point in the  $q$ -cycle has entered a region of negative Jacobian. This bifurcation and the subsequent period-doubling bifurcations are thus related to the noninvertibility of the map.

In summary, the observed behavior agrees with theoretical models of bifurcations near points of resonance, as we have demonstrated for the case of third order. Detailed studies of first, second, and fourth order yielded comparable results. This system serves as an example of how these bifurcations can effect the overall structure in parameter space including the onset of chaos. This first detailed study of these behavior patterns in an experimental system is a key to understanding more complex

nonlinear dynamical systems.

We wish to thank J. Crutchfield, J. Swift, G. Held, J. Testa, and R. Van Buskirk for helpful comments. One of us (C.D.J.) thanks the Miller Institute for Basic Research in Science for support. This work was supported by the U.S. Department of Energy under Contract No. DE-AC03-76SF00098.

---

<sup>1</sup>V. I. Arnold, *Geometrical Methods in the Theory of Ordinary Differential Equations* (Springer-Verlag, New York, 1983), Secs. 21, 34, 35.

<sup>2</sup>V. I. Arnold, *Usp. Mat. Nauk* **27**, No. 5, 119 (1972) [*Russian Math. Surv.* **27**, No. 5, 54 (1972)].

<sup>3</sup>V. I. Arnold, *Funkts. Anal. Prilozh.* **11**, 1 (1977) [*Functional Anal. Appl.* **11**, 85 (1977)].

<sup>4</sup>G. Iooss, *Bifurcations of Maps and Applications* (North-Holland, New York, 1979), p. 105.

<sup>5</sup>F. Takens, *Commun. Math. Inst. Rijksuniv. Utrecht* **3**, 1 (1974).

<sup>6</sup>The negative resistance is produced by a negative-impedance converter. See, for example, P. Horowitz and W. Hill, *The Art of Electronics* (Cambridge Univ., New York, 1980), p. 151.

<sup>7</sup>100 turns No. 28 wire on tape-wound toroidal core of 1 mil Supermalloy (Magnetics 52039-1F), cooled in an ice bath.

<sup>8</sup>C. Grebogi, E. Ott, and J. A. Yorke, *Phys. Rev. Lett.* **48**, 1507 (1982).

<sup>9</sup>This concept was developed independently by J. Swift and K. Wiesenfeld, *Phys. Rev. Lett.* **52**, 705 (1984).